

# Increasing of Aircraft Propeller Efficiency by Using Variable Twist Propeller Blades

Jan Klesa

## Abstract

Numerical iterative method for computation of optimal twist of propeller blades is presented. Incompressible viscous flow and low propeller loading are assumed. Optimal twist of propeller blades dependent on flight velocity and power consumption can be computed using this method. Efficiency of propeller with variable twist varying in presented way is compared with efficiency of conventional constant speed propeller.

## Abstrakt

V článku je představena numerická iterativní metoda pro výpočet optimálního zkroucení vrtulových listů. Předpokládá se nestlačitelné vazké proudění a nízké zatížení vrtule. Pomocí této metody lze vypočítat optimální zkroucení vrtulových listů v závislosti na rychlosti letu a výkonu motoru. Účinnost vrtule s měnitelným zkroucením listů je porovnána s účinností běžné vrtule stálých otáček.

## Nomenclature

$c_D$	drag coefficient of blade section	$T$	thrust
$c_L$	lift coefficient of blade section	$T_c$	thrust coefficient
$c$	blade chord	$V$	freestream velocity
$n_m$	propeller RPM	$W$	local total velocity
$r$	radial coordinate	$\alpha$	angle of attack
$v'$	vortex displacement velocity	$\beta$	blade twist angle
$w_n$	velocity normal to the vortex sheet	$\Gamma$	circulation
$w_t$	tangential velocity	$\varepsilon$	drag to lift ratio
$B$	number of blades	$\zeta$	displacement velocity ratio
$D$	propeller diameter	$\eta$	propeller efficiency
$F$	Prandtl momentum loss factor	$\xi$	nondimensional radius
$G$	circulation function	$\xi_0$	nondimensional hub radius
$P$	power consumed by propeller	$\rho$	air density
$P_c$	power coefficient	$\Phi$	flow angle
$Q$	torque	$\Omega$	propeller angular velocity
$R$	propeller radius		

## 1. Introduction

Smart structures are up-to-date research topic. Compared with classical structures, they can adapt their features according to the changes of operating conditions. Blades of aircraft propellers work from take off to landing under huge variety of conditions. Propeller can't be designed to be optimal under all conditions. Propeller made of smart materials could change its shape according to the operating so that it works with highest possible efficiency and provides considerable increase of efficiency. More information about using smart materials in structure of main helicopter rotor blades can be found in Ref. 11 – 13.

This article contains description of numerical iterative method for computation of optimal twist distribution of propeller blades based on the design procedure described in Ref. 2. If propeller is made of smart material and it can change twist of its blades, results obtained by

this method can be used for design of propeller control system and also for computation of propeller performance.

## 2. Propeller Aerodynamics

System of equations used for design procedure of propeller and for optimalization of propeller twist is described. Equations are based on Ref. 2. Low propeller loading and incompressible flow are assumed. Only brief review of used equations is presented in this paper. For more precise explanation and derivation of equations see Ref. 1 and 2.

### 2.1 Momentum Equations

Thrust of propeller depends on acceleration of the flow passing through the propeller and on the mass flow through the propeller disc. Radial component of induced velocity is denoted  $\Omega r a'$ . Consider element of fluid passing propeller disc through the annulus with inner radius  $r$  and outer radius  $r+dr$ . Freestream velocity (i.e. velocity far in front of the propeller) is  $V$ . According to the momentum theory of propeller (see Ref. 2), the axial component of velocity in the plane of propeller is  $V(1+a)$  and the axial component of velocity far behind propeller is  $V(1+2a)$ . Mass flow through the annulus of the disc is defined by (1).

$$dm = 2\pi r dr \rho V(1+a) \quad (1)$$

Thrust  $dT$  of the annulus can be expressed as  $2VaFdm$ , where  $F$  is momentum loss factor (correction for the momentum losses due the propeller blade tip effect). Thrust acting on the annulus can be expressed by (2).

$$dT = 2\pi r \rho V(1+a)(2VaF)dr \quad (2)$$

According to the momentum theory of propeller (see Ref. 1), radial component of velocity in the plane of the propeller is  $\Omega r(1-a')$  and radial component of velocity far behind the propeller is  $\Omega r(1-2a')$ . Torque needed for rotation of the annulus can be expressed by (3).

$$dQ = 2\pi r \rho V(1+a)(2\Omega r a' F)dr \quad (3)$$

Momentum loss factor was first estimated by Prandtl (see Ref. 8) and later in more accurate form by Goldstein (see Ref. 9).

### 2.2 Circulation Equations

It is assumed that propeller works with minimum induced losses. Betz condition (see Ref. 8) is used for determination of the flow field for minimum induced losses. Lift on the annulus between  $r$  and  $r+dr$  can be expressed as

$$dL = B\rho W\Gamma dr \quad (4)$$

According to Ref. 2, circulation on the annulus between  $r$  and  $r+dr$  is

$$B\Gamma = 2\pi r F w_t \quad (5)$$

where

$$w_t = w_n \cdot \sin \Phi \quad (6)$$

$$v' = \frac{w_n}{\cos \Phi} \quad (7)$$

Velocity ratio  $\zeta$  is defined by (8).

$$\zeta = \frac{v'}{V} \quad (8)$$

Then  $w_t$  can be expressed by (9).

$$w_t = V\zeta \cdot \sin \Phi \cdot \cos \Phi \quad (9)$$

Circulation at radial position  $r$  is

$$\Gamma = \frac{2\pi V^2 \zeta G}{B\Omega} \quad (10)$$

where

$$G = Fx \cdot \cos \Phi \cdot \sin \Phi \quad (11)$$

$$x = \frac{\Omega r}{V} \quad (12)$$

Lift  $dL$  at radius  $r$  is perpendicular to the direction of inflow velocity  $W$  at radius  $r$ . Drag  $dD$  at radius  $r$  is parallel to the direction of inflow velocity  $W$  at radius  $r$ . Thrust  $dT$  and torque  $dQ$  can be expressed using  $dL$  and  $dD$  with formulae (13) and (14).

$$dT = dL \cdot \cos \Phi - dD \cdot \sin \Phi = dL \cdot \cos \Phi \cdot (1 - \varepsilon \tan \Phi) \quad (13)$$

$$\frac{dQ}{r} = dL \cdot \sin \Phi + dD \cdot \cos \Phi = dL \cdot \sin \Phi \cdot \left(1 + \frac{\varepsilon}{\tan \Phi}\right) \quad (14)$$

Where  $\varepsilon$  is drag to lift ratio defined by (15).

$$\varepsilon = \frac{c_D}{c_L} \quad (15)$$

### 2.3 Comparison of Momentum and Circulation Theory

Thrust on the annulus with radius  $r$  and width  $dr$  computed from equations (2) and (13) must be the same. Equation (16) is obtained when equations (2) and (13) are compared.

$$a = \frac{\zeta}{2} \cos^2 \Phi \cdot (1 - \varepsilon \tan \Phi) \quad (16)$$

Torque computed from equations (3) and (14) must be the same. Equation (17) is obtained when equations (3) and (14) are compared.

$$a' = \frac{\zeta}{2x} \cos \Phi \cdot \sin \Phi \cdot \left(1 + \frac{\varepsilon}{\tan \Phi}\right) \quad (17)$$

Flow angle  $\Phi$  can be determined from (18) – see Ref. 2.

$$\tan \Phi = \frac{\left(1 + \frac{\zeta}{2}\right)}{x} \quad (18)$$

According to the Betz condition (see Ref. 8),  $\zeta$  must be constant independent on radius. This is condition for minimum energy loss of the propeller.

### 2.4 Constraint Equations

Nondimensional power and thrust coefficients are defined by (19) and (20).

$$T_c = \frac{2T}{\rho V^2 \pi R^2} \quad (19)$$

$$P_c = \frac{2P}{\rho V^3 \pi R^2} = \frac{2Q\Omega}{\rho V^3 \pi R^2} \quad (20)$$

When equations (19) and (20) are used together with equations (13) and (14), (13) and (14) can be written as (21) and (22).

$$\frac{dT_c}{d\xi} = \frac{dI_1}{d\xi} \cdot \zeta - \frac{dI_2}{d\xi} \cdot \zeta^2 \quad (21)$$

$$\frac{dP_c}{d\xi} = \frac{dJ_1}{d\xi} \cdot \zeta + \frac{dJ_2}{d\xi} \cdot \zeta^2 \quad (22)$$

$I_1, I_2, J_1$  and  $J_2$  are defined by equations (23) to (26).

$$\frac{dI_1}{d\xi} = 4\xi G(1 - \varepsilon \tan \Phi) \quad (23)$$

$$\frac{dI_2}{d\xi} = \lambda \frac{dI_1}{d\xi} \cdot \frac{1}{2\xi} \left( 1 + \frac{\varepsilon}{\tan \Phi} \right) \sin \Phi \cdot \cos \Phi \quad (24)$$

$$\frac{dJ_1}{d\xi} = 4\xi G \left( 1 + \frac{\varepsilon}{\tan \Phi} \right) \quad (25)$$

$$\frac{dJ_2}{d\xi} = \frac{1}{2} \cdot \frac{dJ_1}{d\xi} (1 - \varepsilon \tan \Phi) \cos^2 \Phi \quad (26)$$

$\xi$  is nondimensional radius.

$$\xi = \frac{r}{R} \quad (27)$$

As mentioned before,  $\zeta$  is constant independent on radius. Equations (28) and (29) are obtained after integration of equations (21) and (22).

$$T_c = I_1 \zeta - I_2 \zeta^2 \quad (28)$$

$$P_c = J_1 \zeta + J_2 \zeta^2 \quad (29)$$

$\zeta$  can be easily computed by solving the equations (28) and (29).

$$\zeta = \frac{I_1}{2I_2} - \sqrt{\left( \frac{I_1}{2I_2} \right)^2 - \frac{T_c}{I_2}} \quad (30)$$

$$\zeta = -\frac{J_1}{2J_2} + \sqrt{\left( \frac{J_1}{2J_2} \right)^2 + \frac{P_c}{J_2}} \quad (31)$$

## 2.5 Blade geometry

For blade element at radius  $r$  is the lift per unit length of the blade:

$$\frac{\rho W^2 c c_L}{2} = \rho W \Gamma \quad (32)$$

If  $\Gamma$  from equation (5) is used, (32) can be modified to (33).

$$W c = \frac{4\pi \lambda G V R \zeta}{c_L B} \quad (33)$$

Local total velocity  $W$  can be expressed by (34).

$$W = \frac{V(1+a)}{\sin \Phi} \quad (34)$$

Angle of local blade twist  $\beta$  can be computed from  $\Phi$  and local angle of attack  $\alpha$ .

$$\beta = \alpha + \Phi \quad (35)$$

## 2.6 Momentum Loss Function

Prandtl's momentum loss function is used for the computation (see Ref. 2, 8). Main advantage of this approach is its simplicity. Prandtl's tip loss function is defined by (36).

$$F = \frac{2}{\pi} \arccos(e^{-f}) \quad (36)$$

where

$$f = \frac{B}{2} \cdot \frac{(1-\xi)}{\sin \Phi_t} \quad (37)$$

$\Phi_t$  is flow angle at the blade tip.

$$\tan \Phi_t = \lambda \left( 1 + \frac{\zeta}{2} \right) \quad (38)$$

Then  $\Phi$  can be determined using (39).

$$\tan \Phi = \frac{\tan \Phi_t}{\xi} \quad (39)$$

### 3. Procedure for Propeller Design

#### 3.1 Description of Numerical Method

Design procedure is numerical iterative method based on the procedure described in Ref. 2. Input data necessary for the computation are propeller diameter  $R$ , number of blades  $B$ , air density  $\rho$ , flight velocity  $V$ , angular velocity of the propeller  $\Omega$ , required thrust  $T$  or power consumption  $P$  and characteristics of used airfoils. Numerical procedure consists of following 10 steps:

1. Selection of initial estimate of  $\zeta$  ( $\zeta=0$  was used)
2. Determination of the values of  $F$  and  $\Phi$  for all blade stations using equations (36) to (39)
3. Computation of the product  $Wc$  for selected  $c_L$  from equation (33)
4. Determination  $\varepsilon$  and  $\alpha$  for airfoil section data
5. Computation of  $a$  and  $a'$  and  $W$  from equations (16), (17) and (34)
6. Computation of  $c$  from the product  $Wc$  and  $\beta$  from equation (34)
7. Computation of the derivatives of I and J from the equations (23) to (26) and their numerical integration from  $\xi=\xi_0$  to  $\xi=1$  (i.e. determination of  $I_1, I_2, J_1$  and  $J_2$ )
8. Computation of  $\zeta$  and  $P_c$  from equations (30) and (29) or  $\zeta$  and  $T_c$  from equations (31) and (28)
9. If new value of  $\zeta$  is not enough close to the old one, go to step 2 using new  $\zeta$
10. Computation of propeller efficiency, if wanted, other features can be computed now

Propeller blade was divided into 100 spanwise stations between  $\xi_0$  and  $\xi=1$ . MATLAB code was written for this computation.

#### 3.2 Input Data

Propeller was designed light sports aircraft with engine ROTAX 914 UL. Following input parameters were used:

design velocity	$V_d = 60 \text{ m/s} = 216 \text{ km/h}$
consumed power	$P = 74.5 \text{ kW}$
propeller RPM	$n_m = 2550 \text{ RPM}$
air density	$\rho = 1.225 \text{ kg/m}^3$
number of blades	$B = 3$
diameter	$D = 1.65 \text{ m}$
airfoil	NACA 0009 on the whole propeller blade (i.e. between $\xi=\xi_0$ and $\xi=1$ )
design angle of attack	$\alpha_d = 5^\circ$
inner blade radius	$\xi_0 = 0.2$

#### 4. Procedure for Optimization of Propeller Twist

Optimization procedure uses propeller geometry computed by design procedure. Propeller blade chord distribution remains constant and propeller twist is computed in that way, that the propeller works all the time at highest possible efficiency (Betz condition is used). Numerical procedure for optimization is similar to the design procedure described in chapter 3.1. It also consists from 10 steps:

1. Selection of initial estimate of  $\zeta$  ( $\zeta=0$  was used) – identical to design procedure
2. Determination of the values of  $F$  and  $\Phi$  for all blade stations using equations (36) to (39) – identical to design procedure

3. Computation of the lift coefficient  $c_L$  from equation (33)
  4. Determination  $\varepsilon$  and  $\alpha$  for computed  $c_L$  from airfoil section data
  5. Computation of  $a$  and  $a'$  and  $W$  from equations (16), (17) and (34)
  6. Computation of  $\beta$  from equation (34)
  7. Computation of the derivatives of I and J from the equations (23) to (26) and their numerical integration from  $\zeta=\zeta_0$  to  $\zeta=1$  (i.e. determination of  $I_1$ ,  $I_2$ ,  $J_1$  and  $J_2$ ) – identical to design procedure
  8. Computation of  $\zeta$  and  $P_c$  from equations (30) and (29) or  $\zeta$  and  $T_c$  from equations (31) and (28)
  9. If new value of  $\zeta$  is not enough close to the old one, go to step 2 using new  $\zeta$
  10. Computation of propeller efficiency, if wanted, other features can be computed now
- Whole procedure is done for any desired velocity of flight and power consumption.

## 5. Results of Computation

### 5.1 Geometry of Designed Propeller Blade

Geometry of propeller designed for minimum losses at design point (see chapter 3.2) is presented in following figures. Fig. 5.1 shows nondimensional chord distribution and fig. 5.2 shows blade twist distribution.

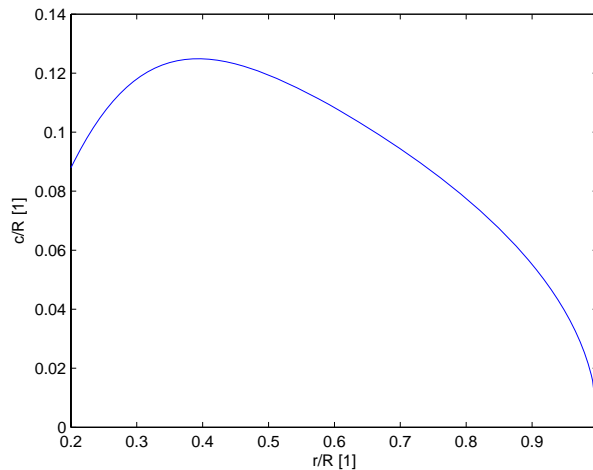


Fig. 5.1 – Nondimensional chord distribution of designed propeller

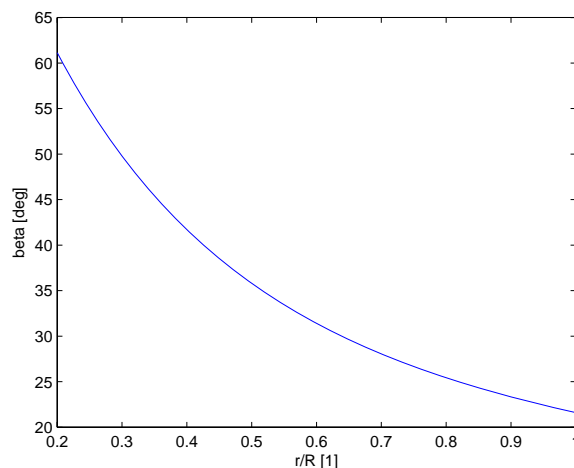


Fig. 5.2 – Twist distribution of designed propeller at design point

### 5.2 Optimization of Propeller for Various Power Consumption and Flight Velocity

Optimization of propeller was done for flight velocities from 20 to 80 m/s (e.g. from 72 to 288 km/h) and for engine power settings 100%, 75%, 55% and 40% of maximum continuous

power (maximum continuous power for engine ROTAX 914 UL equals 74.5 kW). Propeller RPM are assumed to be constant (i.e. 2550 RPM for engine ROTAX 914 UL). Optimal twist distributions for these conditions are in fig. 5.3 to 5.6.

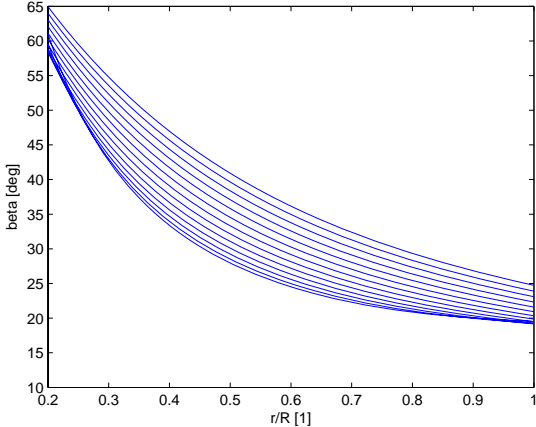


Fig 5.3 – Optimal twist distribution for 100% continuous power, from 20 m/s (the lowest curve) to 80 m/s (the highest curve) with 5 m/s spacing

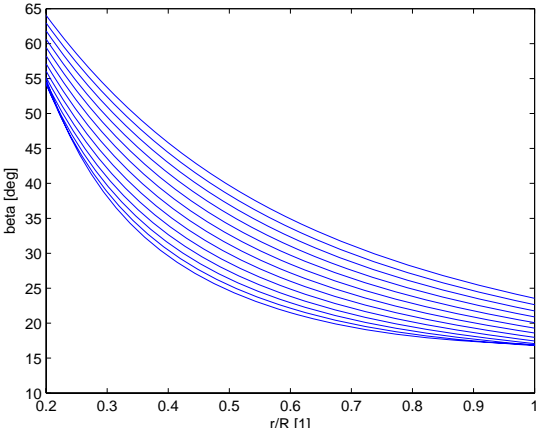


Fig 5.4 – Optimal twist distribution for 75% continuous power, from 20 m/s (the lowest curve) to 80 m/s (the highest curve) with 5 m/s spacing

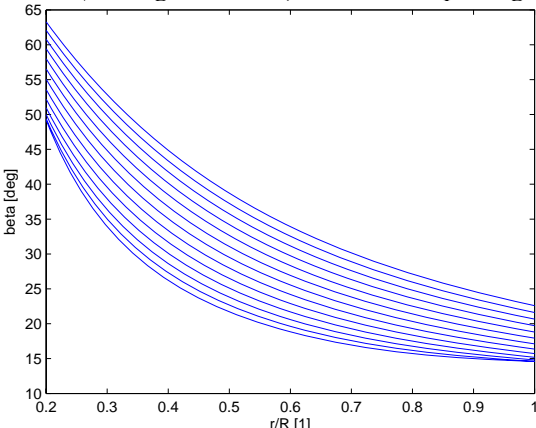


Fig 5.5 – Optimal twist distribution for 55% continuous power, from 20 m/s (the lowest curve) to 80 m/s (the highest curve) with 5 m/s spacing

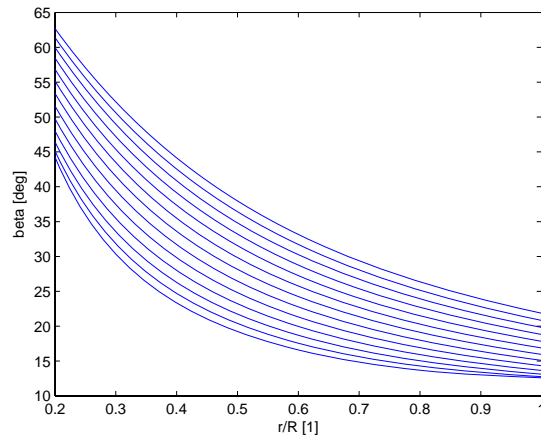


Fig 5.6 – Optimal twist distribution for 40% continuous power, from 20 m/s (the lowest curve) to 80 m/s (the highest curve) with 5 m/s spacing

## 6. Comparison with Conventional Constant Speed Propeller

Constant speed propeller V534BD was used for comparison. Propeller V534BD was designed for engine ROTAX 914 UL and has diameter 1.65 m, so it was designed for the same operating conditions like morphing propeller (see chapter 3.2). Dependence of efficiency on flight velocity (speed ratio  $V/(n*d)$ ) for various power settings can be seen in fig. 6.1 and 6.2 for propeller V534BD and in fig. 6.3 and 6.4 for designed morphing propeller. Characteristics of Propeller V534BD were obtained from results of experiments, Characteristics of morphing propeller were computed by presented numerical method. You can see obvious decrease of efficiency with decreasing power consumption for conventional constant speed propeller (see fig. 6.1 and 6.2). For propeller with ability of morphing twist of propeller blades, efficiency does not decrease for lower power consumption and the efficiency is higher for all flight speeds and power settings. It is possible because of propeller can work permanently in optimal mode due to possibility of twisting propeller blades.

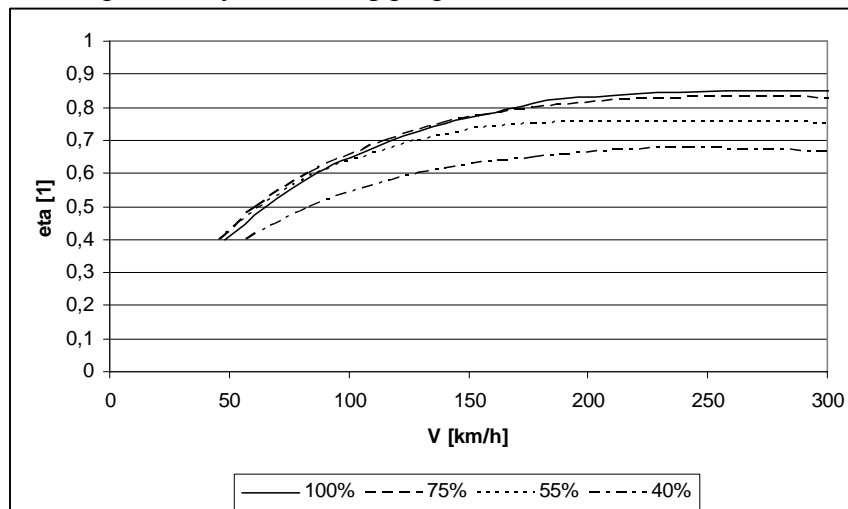


Fig. 6.1 – Dependence of efficiency of propeller V534BD on flight speed for various power settings (engine ROTAX 914 UL, in % of maximum continuous power, i.e. 74,5 kW)

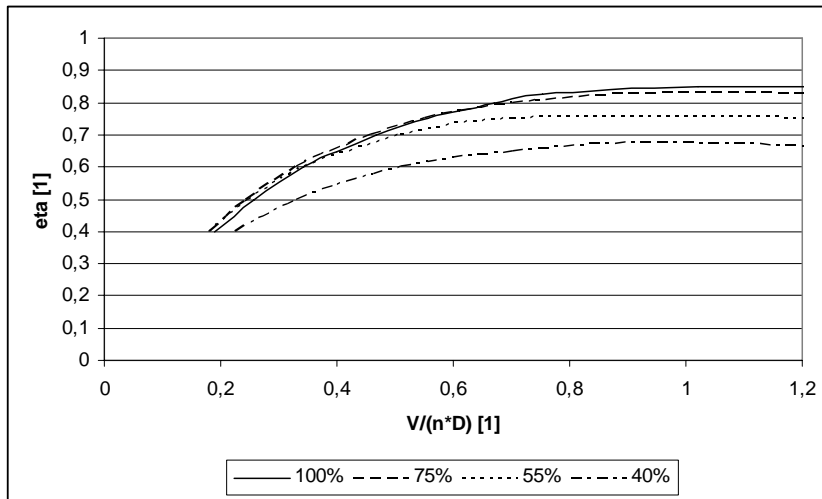


Fig. 6.2 – Dependence of efficiency of propeller V534BD on speed ratio  $V/(n*d)$  for various power settings (engine ROTAX 914 UL, in % of maximum continuous power, i.e. 74,5 kW)

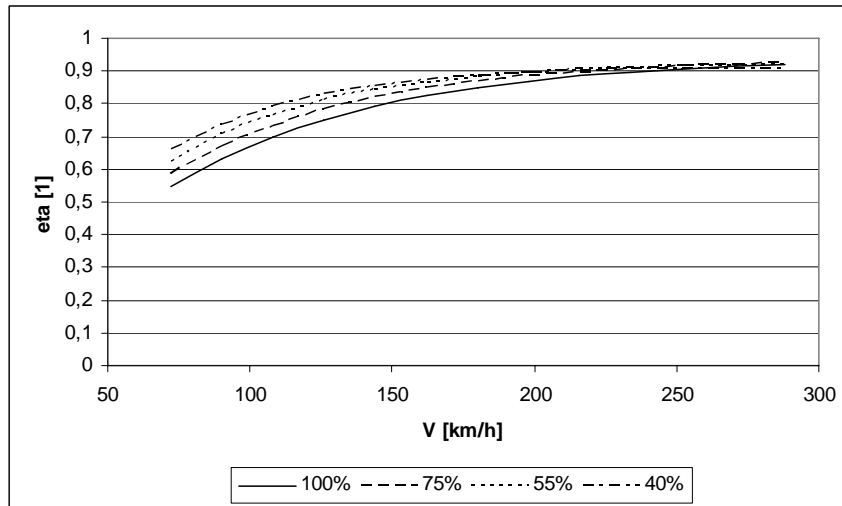


Fig. 6.3 – Dependence of efficiency of morphing propeller on flight speed for various power settings (engine ROTAX 914 UL, in % of maximum continuous power, i.e. 74,5 kW)

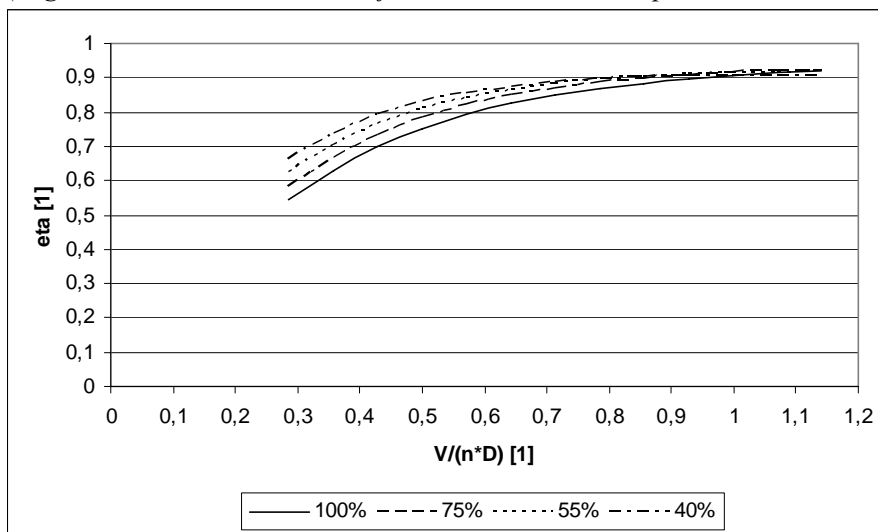


Fig. 6.4 – Dependence of efficiency of morphing propeller on speed ratio  $V/(n*d)$  for various power settings (engine ROTAX 914 UL, in % of maximum continuous power, i.e. 74,5 kW)

## 7. Conclusion and Future Work

Iterative numerical method for computing of optimal twist distribution of propeller blades is presented. It is shown that using variable twist propeller blades leads to significant increase of efficiency. The improvement is especially obvious for lower power loadings (efficiency of the propeller V534BD at 40% of maximum continuous power of engine Rotax 914 UL drops dramatically compared with the 100% case). Future work will be focused on development of method for computation of optimal twist distribution for propellers with high loading.

## 8. References

- [1] Wald, Q. R., The Aerodynamics of Propellers, Progress in Aerospace Sciences, Vol. 42 (2006), pp 85 – 128
- [2] Adkins, C. N., Liebeck R. H., Design of Optimum Propellers, Journal of Propulsion and Power, Vol. 10 (1994), No. 5, pp 676 – 682
- [3] Larrabee, E. E., Practical Design of Minimum Induced Loss Propellers, SAE paper 790585, 1979, Society of Automotive Engineers
- [4] Larrabee, E. E., Five Years Experience with Minimum Induced Loss Propellers – Part I: Theory, SAE paper 840026, Society of Automotive Engineers, 1984
- [5] Larrabee, E. E., Five Years Experience with Minimum Induced Loss Propellers – Part II: Applications, SAE paper 840027, Society of Automotive Engineers, 1984
- [6] Larrabee, E. E., The Screw Propeller, Scientific American, Vol. 243 (1980), No. 1, pp 134 - 148
- [7] Theodorsen T., Theory of Propellers, McGraw-Hill, New York, 1948
- [8] Betz, A., with appendix by Prandtl, L., Luftschrauben mit geringsten Energieverlust, Goettinger Nachrichten, 1919, pp 193 – 217
- [9] Goldstein, S., On the Vortex Theory of Screw Propellers, Proceedings of the Royal Society, Series A, Vol. 123, 1929, pp 440 – 465
- [10] Abbott, I. H., von Doenhoff, A. E., Stivers, L. S., Summary of Airfoil Data, NACA Report No. 824
- [11] Wilbur, M. L. et al, Hover Testing of the NASA/ARMY/MIT Active Twist Rotor Prototype Blade, American Helicopter Society 56<sup>th</sup> Annual Forum, Virginia Beach, VA, May 2-4, 2000
- [12] Straub, F. K. et al, Smart Material-actuated Rotor Technology – SMART, Journal of Intelligent Material Systems and Structures, Vol. 15 (2004), April 2004, pp 249 – 260
- [13] Breitbach, E. J., Smart Structures (Adaptonics) – State of the Art and Future Outlook, in Functional Materials, Wiley-VCH, Weinheim, ISBN 3-527-30254-9